

The conformational phase diagram of charged polymers in the presence of attractive bridging crowders

Kamal Tripathi,^{1,2,3, a)} Hitesh Garg,^{1,2, b)} R. Rajesh,^{1,2, c)} and Satyavani Vemparala^{1,2, d)}

¹⁾ *The Institute of Mathematical Sciences, C.I.T. Campus, Taramani, Chennai 600113, India*

²⁾ *Homi Bhabha National Institute, Training School Complex, Anushakti Nagar, Mumbai 400094, India*

³⁾ *Univ. Grenoble Alpes, CNRS, Grenoble INP, 3SR, F-38000 Grenoble, France*

Using extensive molecular dynamics simulations, we obtain the conformational phase diagram of a charged polymer in the presence of oppositely charged counterions and neutral attractive crowders for monovalent, divalent and trivalent counterion valencies. We demonstrate that the charged polymer can exist in three phases: (1) an extended phase for low charge densities and weak polymer-crowder attractive interactions (*CE*), (2) a collapsed phase for high charge densities and weak polymer-crowder attractive interactions, primarily driven by counterion condensation (*CCI*), and (3) a collapsed phase for strong polymer-crowder attractive interactions, irrespective of the charge density, driven by crowders acting as bridges or crosslinks (*CCB*). Importantly, the simulations reveal that the interaction with crowders can induce collapse, despite the presence of strong repulsive electrostatic interactions, and can replace condensed counterions to facilitate a direct transition from the *CCI* and *CE* phases to the *CCB* phase.

Keywords: polyelectrolyte, crowders, bridging, phase diagram

I. INTRODUCTION

Charged polymers or polyelectrolytes (PEs), are ubiquitous in nature, encompassing biological examples like DNA and proteins, as well as synthetic counterparts such as block copolymers and sodium polystyrene sulfonate etc.^{1–9}. The conformations of highly charged PEs are influenced by a combination of factors, including long-range electrostatic interactions, counterion entropy, solvent quality, temperature, counterion valency, and dielectric constant of the solvent, which are reasonably well-understood^{10–14}. With increase in PE backbone charge density, the oppositely charged counterions begin to condense onto the PE via Manning condensation^{15,16}. Beyond a critical charge density, the PE undergoes a transition from an extended to a collapsed conformation, irrespective of solvent quality^{17–29}. Several mechanisms, such as ionic solid theory, dipole theory, and counterion fluctuation theory, have been proposed to explain various aspects of the counterintuitive collapse behavior of like-charged PEs^{15,17–23,25,27,28,30–38}.

While the conformations of an isolated PE have been studied in detail, it is important to consider that PEs often exist within complex and crowded heterogeneous environments^{39–45}. In such environments, the conformational landscape of even neutral polymers is significantly altered by the presence of crowder molecules, which can induce novel phases such as bridging and depletion-induced collapsed phases (see details below) through spe-

cific or non-specific interactions^{46–54}. It is, thus, reasonable to expect that crowders will also affect the conformations of a PE, as the relative strength of the polymer-crowder interactions and electrostatic interactions is varied. Although few prior studies^{55,56} have shown that the inclusion of crowder molecules stabilize the crowder-free equilibrium collapsed conformations of small charged or overall charge-neutral polymers, the specific mechanisms underlying crowder-polymer interactions and the intricate interplay between counterions and crowders remain unexplored. Thus, despite the widespread applications, a comprehensive understanding of how both crowders and counterions influence PE conformations is currently lacking and constitutes the central focus of this paper.

Unlike the case of PEs, the effect of crowders on the conformations of neutral polymers is better studied. When the polymer-crowder interactions are purely repulsive, entropic effects can induce effective depletion induced attractive interactions between the monomers which in turn drive a collapse transition^{40,53,54,57–61}. The depletion effects are enhanced with further attractive interaction among the crowders⁶². When the interactions between the polymer and the crowders exhibit weak attraction, the crowders assume the role of a typical good solvent, leading to a preference for extended polymer conformations. However, on further increase of polymer-crowder attractive interactions, a counterintuitive collapse transition (effective poor solvent condition) is observed even for a self-avoiding polymer where the crowders act as bridges or crosslinks between monomers.^{62–66} Recently, we obtained the detailed configurational phase diagram of neutral polymers in the presence of attractive crowders, by delineating phase transitions from extended conformations to collapsed conformations induced by both intra-polymer attraction and bridging effects due to crowders⁶².

^{a)} Electronic mail: kamalt@imsc.res.in

^{b)} Electronic mail: hiteshgarg@imsc.res.in

^{c)} Electronic mail: rrajesh@imsc.res.in

^{d)} Electronic mail: vani@imsc.res.in

The effect of crowders on the conformation of PEs is of considerable interest in the context of membraneless biomolecular condensates^{67–70}. These condensates form due to either polymer polymer phase separation (PPPS) or liquid liquid phase separation (LLPS), both driven by strong attractive interaction with crowders. Studied primarily from the perspective of chromatin organization, these two mechanisms of phase separation mainly differ in the relative strengths of chromatin-chromatin interactions and chromatin-crowder interactions. PPPS is driven by formation of bridges or cross links between distant parts along chromatin mediated by crowder molecules, thus generating a collapsed globule conformation. The bridging crowders do not undergo a phase separation in the absence of attractive interaction with chromatin. LLPS, on the other hand, leads to condensates resembling liquid-like crowder-chromatin droplets. Unlike PPPS, the crowders phase separate even in the absence of chromatin. There are experimental and theoretical studies investigating the role of bridging interactions in chromatin reorganization via PPPS or LLPS^{71–79}. However, despite chromatin being inherently a charged polymer, it is usually modeled as a coarse-grained neutral polymer in the presence of neutral crowders, thus ignoring the presence of charged counterions and long range interactions^{71–74,77}. A study of PE in a crowded environment, provides a more realistic model for biopolymers such as chromatin and also makes it possible to investigate phenomena such as PPPS arising due to competing interactions with counterions and crowders.

In this paper, we investigate the impact of attractive neutral crowders on the conformations of a single, similarly charged PE in the presence of oppositely charged counterions. We employ extensive molecular dynamics simulations utilizing generic coarse-grained bead-spring models. We identify three distinct phases: (1) the *CCI* phase, which corresponds to a collapsed state primarily driven by the condensation of counterions; (2) the *CE* phase, characterized by an extended conformation of the polymer due to repulsive electrostatic interactions within the PE; and (3) the *CCB* phase, representing a secondary collapsed state primarily induced by the presence of attractive bridging crowders, with a substantial number of crowders located within the collapsed conformation. By identifying the phase transitions among these phases, we obtain the phase diagram in the PE charge density and polymer-crowder interaction phase space for monovalent, divalent, and trivalent counterions.

II. MODEL AND METHODS

We model a flexible PE chain using a coarse-grained linear bead-spring model consisting of N_m monomers of charge $-q$ (measured in units of e) linked together by harmonic springs with bond interaction energy

$$U_{bond}(r) = \frac{1}{2}k(r - r_0)^2, \quad (1)$$

TABLE I. Parameters for the LJ potential [see Eq. (2)] between different pairs of particles. The notations m , i and c represent monomers, counterions and crowders respectively.

pair	ϵ	σ	r_c
$m - m$	1.0	1.0	$2^{1/6}$
$i - i$	1.0	1.0	$2^{1/6}$
$m - i$	1.0	1.0	$2^{1/6}$
$m - c$	ϵ_{mc}	1.0	2.5
$i - c$	1.0	1.0	$2^{1/6}$
$c - c$	1.0	1.0	2.5

where k is the spring constant, r_0 is the equilibrium bond-length and r is the distance between two bonded monomers. We set $r_0 = 2^{1/6}\sigma$, $k = 500k_B T\sigma^{-2}$, where σ is the size of the monomer in Lennard Jones (LJ) units (see below), k_B is the Boltzmann’s constant and T is the temperature. N_m/Z neutralizing counterions with charge $+Zq$, each of the same size and mass as the monomer, are added to the system, where Z is the valency of the counterion ($Z = 1, 2, 3$). In addition, N_c neutral crowders, of same size and mass as the monomer, are added such that the number density of the crowders is $\rho_c = N_c/L^3 = 0.05\sigma^{-3}$, where L is the size of the simulation box. The monomer density is fixed at $N_m/L^3 = 1.112 \times 10^{-3}\sigma^{-3}$. For this box length, the PE chain in its extended phase does not interact with its own periodic images.

Non-bonded pairs of particles interact via excluded volume interactions (PE monomers, counterions, crowders) as well as long ranged electrostatic interactions (PE monomers, counterions). The excluded volume interactions are modeled by the truncated and shifted LJ potential,

$$U_{jk}(r) = 4\epsilon_{jk} \left[\left(\frac{\sigma}{r} \right)^{12} - \left(\frac{\sigma}{r} \right)^6 \right], \quad r < r_c^{jk}, \quad (2)$$

where indices j and k can be m (monomer), i (counterion) or c (crowder), and r is the distance between two particles. The parameter ϵ_{jk} and cutoff r_c^{jk} are pair-dependent while σ is same for all particles. The LJ parameters for the different pairs are listed in Table I. Other than $m-c$ and $c-c$ pairs, all other pair interactions are purely repulsive. In particular, this choice mimics an implicit good solvent condition for the polymer.

The PE, counterions, and crowders are assumed to be in a medium of uniform relative dielectric constant ϵ . The electrostatic energy between any two charges q_1 and q_2 separated by distance r is given by

$$U_C(r) = \frac{q_1 q_2}{4\pi\epsilon\epsilon_0 r}, \quad (3)$$

where ϵ_0 is the dielectric permittivity of vacuum. The relative strength of electrostatic interactions among charged monomers along the PE chain is characterized by a di-

mensionless parameter A :

$$A = \frac{q^2 \ell_B}{r_0}, \quad \ell_B = \frac{e^2}{4\pi\epsilon\epsilon_0 k_B T}, \quad (4)$$

where ℓ_B is the Bjerrum length³⁵ at which the electrostatic energy between two elementary charges e is comparable to the thermal energy $k_B T$. The strength of electrostatic interactions, A , can be tuned by either changing q while keeping ϵ fixed or by changing ϵ while keeping q fixed. In our simulations, we systematically scale the monomer charges q to vary A . For $Z = 1, 2, 3$, we do simulations for A/A_c ranging from 0.001 to 2.0, where A_c is the critical charge density for a PE in a good solvent in the absence of crowders. For each value of A , a range of values of ϵ_{mc} are explored. Lengths, temperatures and times are given in units of σ , ϵ/k_B , and $\sqrt{m\sigma^2/\epsilon}$ respectively.

All the simulations are carried out using the molecular dynamics simulation package LAMMPS⁸⁰ in NVT ensemble with periodic boundary conditions. The equations of motion are integrated using the velocity-Verlet algorithm^{81,82} with a time step of 0.001. The system is initially equilibrated for 10^6 steps and the analyses are done over subsequent 10^7 steps. The temperature is maintained through a Nosé-Hoover thermostat^{83,84}. The long ranged Coulomb interactions are evaluated using the particle-particle/particle-mesh (PPPM) technique⁸⁵.

III. RESULTS

A. Collapse transition in PEs with crowder interactions

Before investigating the influence of attractive neutral crowders on the conformational behavior of charged PEs, we first determine the critical charge density, A_c , for the extended-collapsed transition of a single PE in good solvent conditions, in the absence of crowders. To determine A_c , we monitor the radius of gyration, R_g , as a function of A , for all the three counterion valencies. R_g is defined as

$$R_g^2 = \frac{1}{2N_m^2} \sum_{j=1}^{N_m} \sum_{k=1}^{N_m} |\vec{r}_j - \vec{r}_k|^2, \quad (5)$$

where \vec{r}_i denotes the position vector of the i -th monomer. The variation of R_g with A for two different values of N_m is shown in Fig. 1. By identifying the collapsed phase to be the regime where the data for $R_g/N_m^{1/3}$ collapse onto one curve, we obtain $A_c \approx 9.5, 4.0, 2.0$ for $Z = 1, 2, 3$ respectively. These values are larger than those obtained earlier for the PE in poor solvent conditions¹⁷.

Our aim is to identify the different phases and obtain the phase diagram of the PE in the presence of attractive crowders, particularly in the A - ϵ_{mc} phase space. Towards this end, we determine R_g and asphericity, α , at

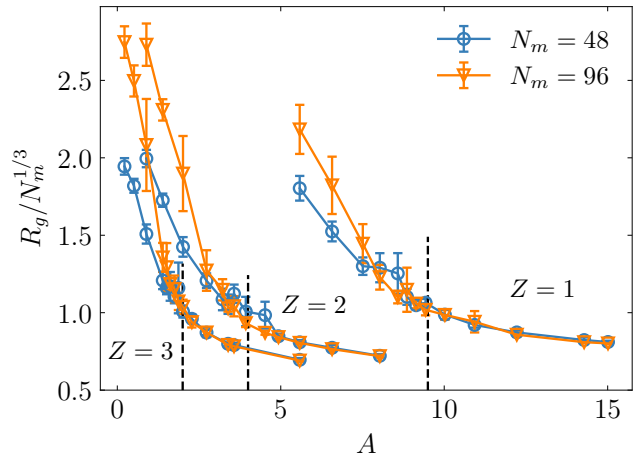


FIG. 1. The variation of radius of gyration, R_g , with charge density A for two lengths of the PE, $N_m = 48, 96$, in the absence of crowders. The collapsed phase is identified to be the regime when the data for $R_g/N_m^{1/3}$ collapse on top of each other. The vertical dashed lines correspond to 2.0, 4.0, 9.5 and are identified as approximate values of A_c .

different attractive strengths, ϵ_{mc} , for a range of values of A/A_c . Asphericity, α , is defined as^{86–88}

$$\alpha = \frac{\lambda_1 \lambda_2 + \lambda_2 \lambda_3 + \lambda_3 \lambda_1}{(\lambda_1 + \lambda_2 + \lambda_3)^2}, \quad (6)$$

where $\lambda_1, \lambda_2, \lambda_3$ are the eigenvalues of the moment of inertia tensor and the value of α varies between 0 (sphere) and 1 (rod).

We first focus on $A/A_c < 1$ (partial counterion condensation regime), where in the absence of crowders, the PE is in an extended conformation, the CE phase, due to intra polymer electrostatic repulsion. Consider the case of trivalent counterions, shown in Fig. 2 (a). When the crowder strength ϵ_{mc} is relatively small, the value of R_g closely resembles that observed without crowders, thus maintaining the extended conformation of the PE. However, as ϵ_{mc} increases further, a rapid reduction in R_g is observed, indicating a pronounced collapse of the PE. Concurrently, the asphericity of the PE diminishes from a value close to 0.5 to near zero, consistent with expectations for a collapsed phase, as depicted in Figure 2 (b). To understand the origin of this attractive crowder induced collapse of PE, we examine the radial density distribution of crowders, $\rho_c(r)$, measured from the center of mass of the PE in the collapsed phase ($\epsilon_{mc} = 4.0$). Fig. 3 shows an excess crowder density within the collapsed PE region compared to the exterior, indicating that the collapse can be primarily attributed to bridging interactions with crowders rather than depletion effects. This specific collapsed phase, triggered by bridging interactions with neutral crowders, will be referred as the CCB (bridging-induced collapsed) phase. Further evidence of the PE being collapsed for large ϵ_{mc} can be seen

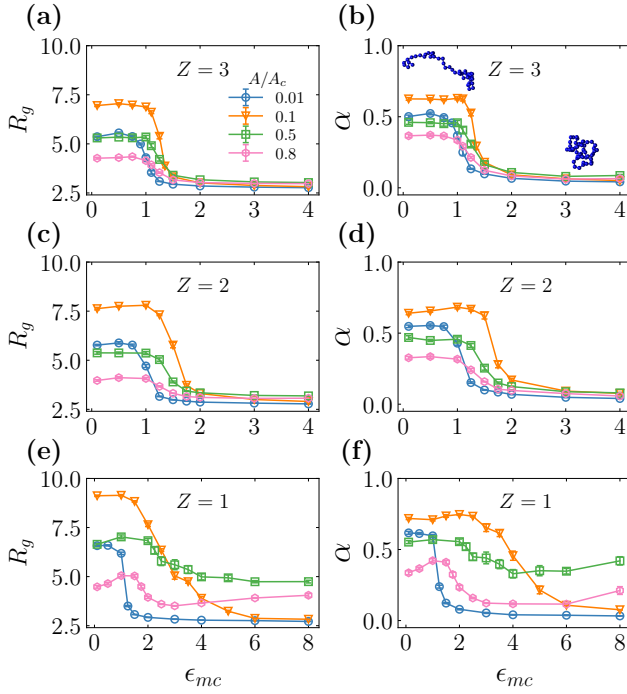


FIG. 2. $A/A_c < 1.0$: The radius of gyration, R_g , of the PE chain and asphericity α as a function of ϵ_{mc} for (a, b) $Z = 3$, (c, d) $Z = 2$, (e, f) $Z = 1$, and $N_m = 48$.

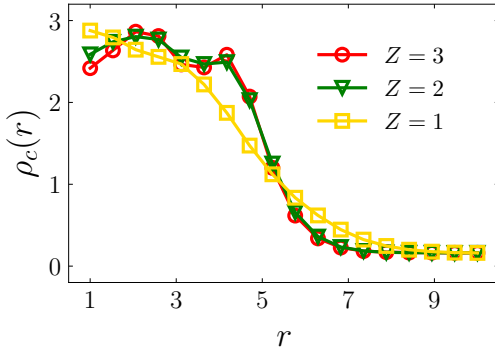


FIG. 3. $A/A_c = 0.1$: Radial density function of crowders $\rho_c(r)$ measured from the center of mass of the collapsed PE chain for all the three valencies of counterions for $\epsilon_{mc} = 4.0$.

from the data collapse of $R_g/N_m^{1/3}$, for two different PE chain lengths, in Fig. S1 (see Supp Info). We can thus identify a critical ϵ_{mc}^* , for each $A/A_c < 1$, beyond which an extended to collapsed transition (*CE-CCB*) is driven by bridging neutral crowders. This allows us to construct the *CE-CCB* phase line in Sec. III B. Similar trends are seen for divalent counterions as well [see Fig. 2(c),(d)].

The dependence of R_g on ϵ_{mc} for monovalent counterions exhibits distinct characteristics compared to PEs with divalent and trivalent counterions, as shown in Fig. 2 (e). While the behavior of R_g for monovalent counterions at $A/A_c = 0.01$ and 0.1 is similar to that of divalent and

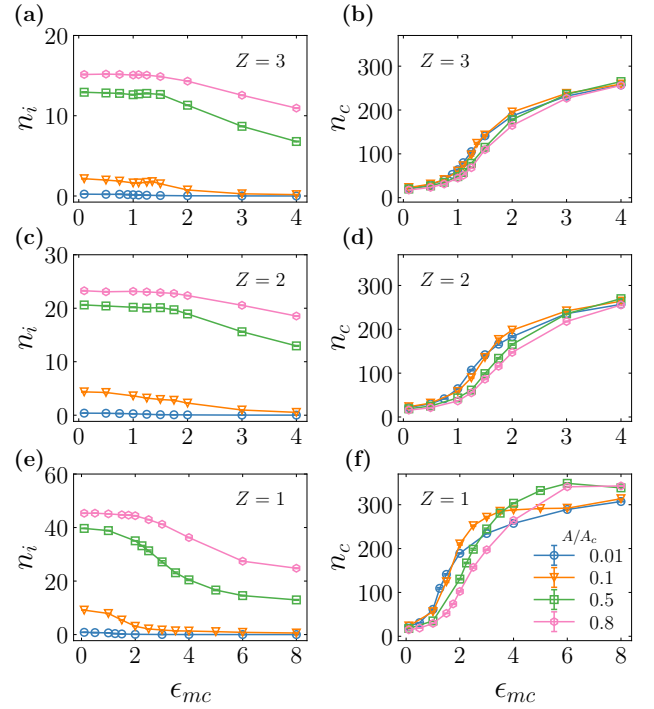


FIG. 4. The number of condensed counterions, n_i , and condensed crowders, n_c , within a distance 2σ of the PE chain as a function of ϵ_{mc} for $A/A_c < 1.0$ for (a, b) $Z = 3$, (c, d) $Z = 2$, (e, f) $Z = 1$.

trivalent counterions, the transition occurs at larger critical values of ϵ_{mc}^* . In contrast, for $A/A_c = 0.5$ and 0.8 , the increase in ϵ_{mc} does not lead to a significant reduction in R_g . Moreover, the corresponding asphericity remains significantly different from zero even at large ϵ_{mc} values, as illustrated in Fig. 2 (f). Taken together, this suggests that the PE does not undergo collapse for intermediate A values in the presence of monovalent counterions. We discuss the implications of this feature for the phase diagram for monovalent counterions in Sec. III B.

To understand the interplay between the condensed counterions and crowders as a function of increased monomer-crowder interaction strength, we calculate their numbers, n_i and n_c within a distance of 2σ of any monomer. In the regime of very low A values, where Manning condensation has yet to take effect, n_i remains close to zero across all ϵ_{mc} values, while n_c exhibits an increase that eventually saturates at larger ϵ_{mc} values, for $Z = 1, 2, 3$, as depicted in Fig. 4. While the behavior of n_c is largely unaffected by variations in A/A_c , a clear reduction in the number of condensed counterions with increasing ϵ_{mc} is observed for values of $A/A_c \lesssim 1$. A consequent increase in repulsive electrostatic energy, due to loss of charge renormalizing counterions, is however compensated by the increased attractive van der Waal energy due to neutral crowders, as can be seen from Fig. S2, and drives the collapse of PE.

We now focus on the results for $A/A_c > 1$, where in

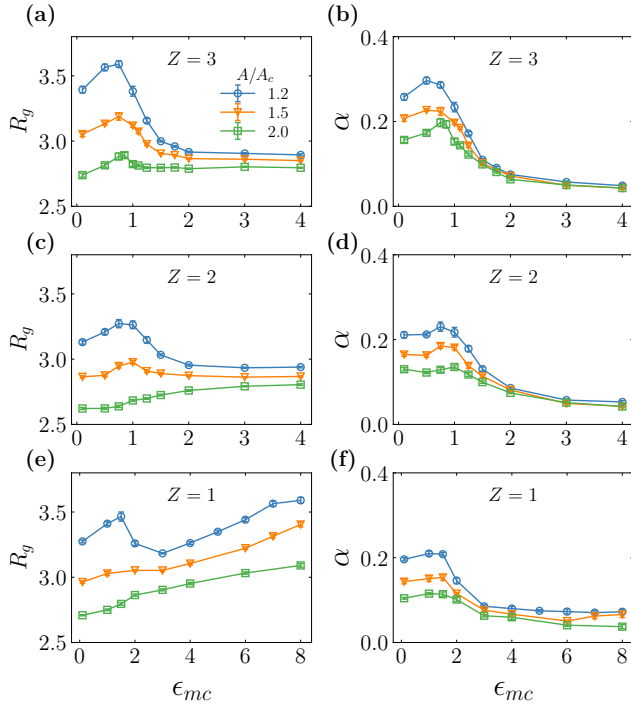


FIG. 5. $A/A_c > 1.0$: The radius of gyration, R_g , of the PE chain and asphericity α as a function of ϵ_{mc} for (a, b) $Z = 3$, (c, d) $Z = 2$, (e, f) $Z = 1$, and $N_m = 48$.

the absence of crowders, complete counterion condensation occurs and the PE is in a collapsed conformation. Consider first the case for trivalent counterions. When ϵ_{mc} is increased from zero, an increase of R_g can be seen from Fig. 5(a) suggesting swelling of the collapsed conformation. For this range of ϵ_{mc} values, the crowders effectively act as good solvent conditions and the swelling can be attributed to enhanced attractive interaction energy between PE and crowders. For larger values of ϵ_{mc} , the R_g saturates to a value that is independent of value of ϵ_{mc} . Throughout this entire range of ϵ_{mc} , R_g consistently maintains values significantly smaller than those corresponding to the extended phase of the PE for $A/A_c < 1$ (as seen in Fig.2(a)), demonstrating that the PE retains a collapsed conformation. This is further supported by the consistently low values of the asphericity, α , shown in Fig.5(b). In order to quantitatively validate the collapsed state of the PE across the entire ϵ_{mc} range, Fig.6(a) illustrates the data collapse of R_g onto one curve for two distinct system sizes when scaled by $N_m^{1/3}$. Similar trends are observed for both divalent (see Fig.5(c-d)) and monovalent (see Fig.5(e-f)) counterions.

With the understanding that the PE consistently maintains a collapsed conformation across the entire range of ϵ_{mc} values, we now probe whether the nature of this collapsed phase remains uniform throughout. Snapshots of the PE (blue color particles), along with counterions (lime green particles) and crowders (golden yellow particles) within a distance of 2σ from the PE, are shown

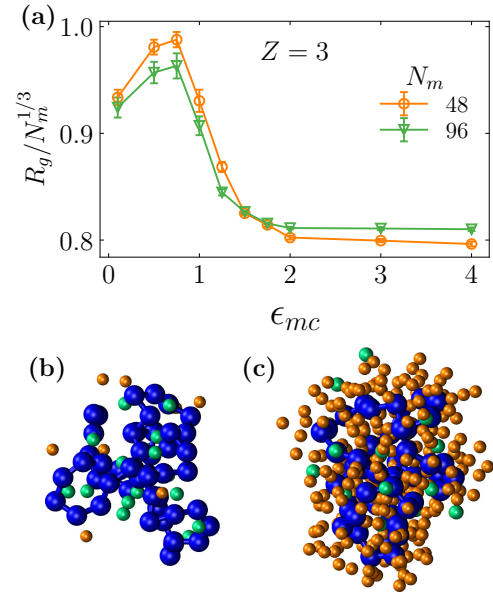


FIG. 6. (a) The scaled R_g for two different $N_m = 48, 96$ for $A/A_c = 1.2$ and $Z = 3$. (b-c) Snapshots of typical configurations for $N_m = 48$ and $Z = 3$ with $A/A_c = 1.2$ for (b) $\epsilon_{mc} = 0.1$ and (c) $\epsilon_{mc} = 3.0$. The monomers, counterions and crowders are colored by blue, lime green, and golden yellow respectively.

in Fig.6(b-c) for both small and large ϵ_{mc} values. In the case of small ϵ_{mc} , the collapsed phase lacks crowders within the globule, forming what we refer to as the *CCI* phase. In contrast, for large ϵ_{mc} , a significant number of crowders are enclosed within the globule, defining the *CCB* phase, as discussed previously. To differentiate between these two collapsed phases (*CCI* and *CCB*), we analyze the radial density distribution of the crowders from the center of the collapsed globule, $\rho_c(r)$, as shown in Fig.7. For all counterion valencies, it can be seen that the crowders are depleted from the center of the collapsed globule under small ϵ_{mc} conditions (*CCI* phase), in contrast to the bulk crowder density ($\rho_c^{bulk} = 0.05$). In contrast, for large ϵ_{mc} values (*CCB* phase), a pronounced crowder overpopulation is observed within the globule ($\rho_c^{center} \approx 2.5$), strongly indicating that the two collapsed phases are distinct.

To identify the transition between the two collapsed *CCI* and *CCB* phases, we define a mean density of crowders within the collapsed phase, $\bar{\rho}_c$, as the density within a radius $R_g/2$. As can be seen from the right panels of Fig. 7, $\bar{\rho}_c$ remains close to zero for small ϵ_{mc} values across all counterion valencies, then sharply increases beyond a critical threshold ϵ_{mc}^* . Remarkably, the $\bar{\rho}_c$ data exhibits minimal dependence on A/A_c , implying that the critical ϵ_{mc}^* is relatively independent of A for $A/A_c > 1$. We now ask whether the introduction of crowders leads to the displacement of condensed counterions from the *CCI* phase, as a function of ϵ_{mc} ? For all counterion valencies, even

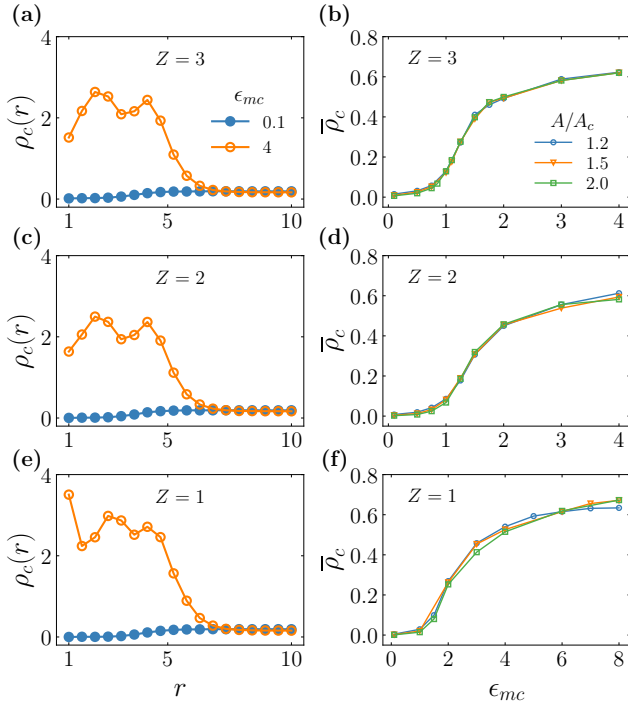


FIG. 7. Radial density function of crowders $\rho_c(r)$ measured from the center of mass of the collapsed PE chain for all the three valencies of counterions considered in the study for $\epsilon_{mc} = 0.1, 4$. The data shown in this figure is for system with crowder density $\rho_c = 0.05$ and $A/A_c = 2.0$. The critical Radial density function $\rho_c(r)$ of crowders within collapsed conformation for all the three valencies of counterions considered in the study as a function of ϵ_{mc} . The transition from *CCI*–*CCB* phase is identified *via* this parameter. The data shown in this figure is for system with crowder density $\rho_c = 0.05$.

though A is large, as ϵ_{mc} is increased counterions are expelled from the PE globule, as can be seen from the variation of n_i with ϵ_{mc} in Fig. 8. Correspondingly, the number of condensed crowders, n_c increases sharply to compensate for the increased electrostatic repulsion (see right panels of Fig. 8). It is worth noting that the number of condensed crowders, n_c , exceeds that of the displaced counterions by an order of magnitude. The consequent increase in electrostatic energy is compensated by the attractive van der Waal energy as can be seen from Fig. S3.

B. Conformational phase diagram of PEs with crowder interactions

In Sec. IIIA, we showed that PE can exist in three phases in the presence of neutral crowders. (1)*CE*: extended conformations for low charge density, below a critical value, and weak PE–crowder attractive interactions, (2)*CCB*: collapsed conformations for charged den-

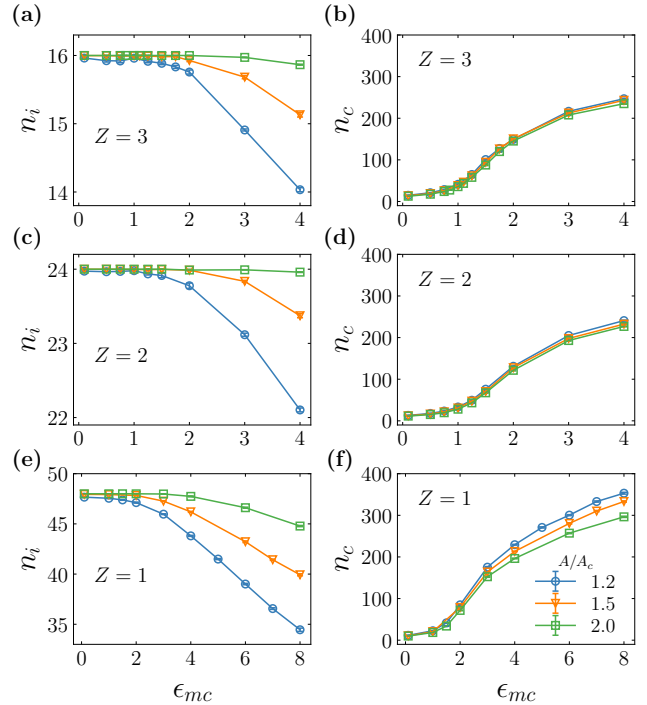


FIG. 8. The number of condensed counterions, n_i , and condensed crowders, n_c , within a distance 2σ of the PE chain as a function of ϵ_{mc} for $A/A_c > 1.0$ for (a, b) $Z = 3$, (c, d) $Z = 2$, (e, f) $Z = 1$.

sity values less than or near the critical value and for strong PE–crowder attractive interactions, and (3)*CCI*: collapsed conformations for charged density values higher than the critical value, primarily due to counterion condensation. We now explore the complete phase diagram of the system in A – ϵ_{mc} plane and demarcate the phase boundaries.

We choose two different parameters to locate the phase boundaries among the three phases *CE*–*CCB* and *CCI*–*CCB*. Similar to our previous work⁶², variation of R_g with ϵ_{mc} curves for various values of A/A_c will be used for *CE*–*CCB* phase boundary as follows. A curve from R_g vs ϵ_{mc} plot is chosen which represents a specific A/A_c value. This curve is then fitted to a general hyperbolic tangent function ($R_g(\epsilon_{mc})$). The first derivative $dR_g/d\epsilon_{mc}$ gives the rate of change of R_g with respect to ϵ_{mc} . Solving $dR_g/d\epsilon_{mc} = 0$ yields the value ϵ_{mc}^* for which the rate of change of R_g with respect to ϵ_{mc} is maximum. The value of ϵ_{mc}^* indicates the location of phase boundary between two phases on either side of ϵ_{mc} . This process is repeated for all the different value of A/A_c . However, for obtaining the *CCI*–*CCB* phase boundary, R_g is not a good parameter as it does not vary much across the two collapsed phases. On the other hand, the parameter $\bar{\rho}_c$ clearly distinguishes between the two collapsed phases, as can be seen from Fig. 7 and we use it to identify the *CCI*–*CCB* phase boundary. Similar to how we analyzed R_g to determine the phase boundary between *CE*–*CCB*,

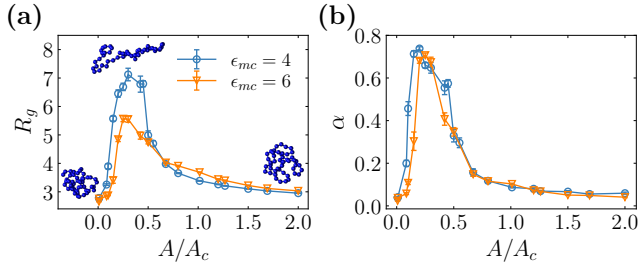


FIG. 9. $Z = 1$: The variation of (a) R_g and (b) α with A/A_c for fixed $\epsilon_{mc} = 4, 6$. The snapshots in (a) correspond to $\epsilon_{mc} = 4.0$.

we pinpoint the critical value of ϵ_{mc}^* for the *CCI-CCB* phase transition by identifying the point at which the rate of change of $\bar{\rho}_c$ with respect to ϵ_{mc} is maximized. To determine the *CE-CCI* phase boundary, we simulate the PE for $N_m = 48, 96$, and identify the critical value of A to be that value beyond which the data for $R_g/N_m^{1/3}$ collapse onto one curve.

The phase diagram in the $A-\epsilon_{mc}$, thus obtained from the two analysis described above, can be seen in Fig. 10. For all the three counterion valencies, the three direct phase transitions *CE-CCI*, *CE-CCB*, and *CCI-CCB* are possible. However, for monovalent counterions, for the range of ϵ_{mc} considered, there is no *CE-CCB* phase transition for intermediate values of A . This implies that, for fixed $\epsilon_{mc} \gtrsim 2$ and increasing A/A_c , we expect a reentrant *CCB-CE-CCB* phase transition. If this were the case, then if the system is simulated at a fixed large ϵ_{mc} and by increasing A , the PE should undergo collapsed-extended-collapsed transitions. The results for such simulations are shown in Fig. 9. For intermediate values of A/A_c , the PE is extended, as can be seen from the snapshot, with a corresponding large value of R_g compared to small and large A/A_c [see Fig. 9(a)]. For small and large A/A_c , the PE is collapsed as can be seen from both the snapshots [see Fig. 9(a)], as well as asphericity being close to zero [see Fig. 9(b)]. Thus we confirm that for intermediate A/A_c , attractive crowders are unable to drive an extended to collapsed transition.

We also observe that the critical value ϵ_{mc}^* for the *CCI-CCB* phase transition is largely independent of A . This is surprising, as one would expect that for higher values of parameter A , the *CCI* phase's stability would strengthen, necessitating a correspondingly larger ϵ_{mc} to induce its destabilization. A discussion of the implications for the different theories of PE can be found in Sec. IV. Further, the *CE-CCI* phase boundary is largely independent of ϵ_{mc} for small ϵ_{mc} and occurs around $A/A_c \approx 1$. This is to be expected as the transition is driven by condensed counterions, and crowders do not play any significant role. For intermediate values of ϵ_{mc} , the presence of crowders decreases A_c .

IV. DISCUSSION AND CONCLUSION

The notion of macromolecular crowding in cellular environments affecting the stability of biopolymers, such as proteins, is now well-known^{89,90}. However, most of the studies on crowders treat the crowders as hard particles, whose primary mode of interaction with proteins or model polymers is via depletion: the entropically driven exclusion of repulsive crowders leads to the collapse of the polymer/protein. Only recently, the role of soft attractive interactions between polymers and crowders has been explored, and it has been implicated in various phenomena such as chromosome organization, LLPS (liquid-liquid phase separation), etc^{67-74,77}. Simple polymer models have been effectively used to understand the role of soft attractive interactions between crowders and biopolymers like chromatin, demonstrating their impact on the conformational landscape. These studies have investigated the influence of both attractive polymer-crowder interaction energy and crowder density. However, it should be noted that most of these models are based on neutral polymers, and their relevance to inherently charged biopolymers remains unclear.

Like-charged polymers, polyelectrolytes(PE), have been shown to undergo a counterintuitive extended to collapsed transition, in the presence of oppositely charged counterions, when the charge density of the backbone, A , is larger than a critical value A_c ¹⁷⁻²⁹. This dependence of the PE conformations on A suggests an analogy with monomer-monomer interaction energy (ϵ_{mm}) in neutral polymers, where small and large ϵ_{mm} values correspond to extended and collapsed states, respectively. Recently, we obtained a detailed phase diagram for neutral polymers in the presence of attractive crowders in the $\epsilon_{mm}-\epsilon_{mc}$ phase, where ϵ_{mc} represents the polymer-crowder interaction strength⁶². In this paper, we explored the conformations of PEs in the $A-\epsilon_{mc}$ phase space. We addressed the following questions: (1) Do neutral crowders differentially affect the conformations of PE, depending on the charge density of the PE (A)? (2) What is the role of the valency (Z) of the counterions? (3) What is the conformational phase diagram of PE in the $A-\epsilon_{mc}$ phase space? (4) How do attractive crowders impact charged polymers compared to neutral polymers?

We demonstrate that attractive neutral crowders have the ability to collapse a charged extended polymers, despite the inherent repulsive interactions arising from like charges. This collapse phenomenon occurs for all counterion valencies. We show the existence of three distinct phases in the $A - \epsilon_{mc}$ phase space: (1) An extended phase denoted as *CE*, observed for low charge densities and weak polymer-crowder attractive interactions. For monovalent counterions, the *CE* also exists for strong polymer-crowder attractive interactions. (2) A collapsed phase labeled as *CCI*, observed for high charge densities and weak polymer-crowder attractive interactions, primarily driven by the condensation of counterions within the polymer structure. (3) A collapsed phase denoted

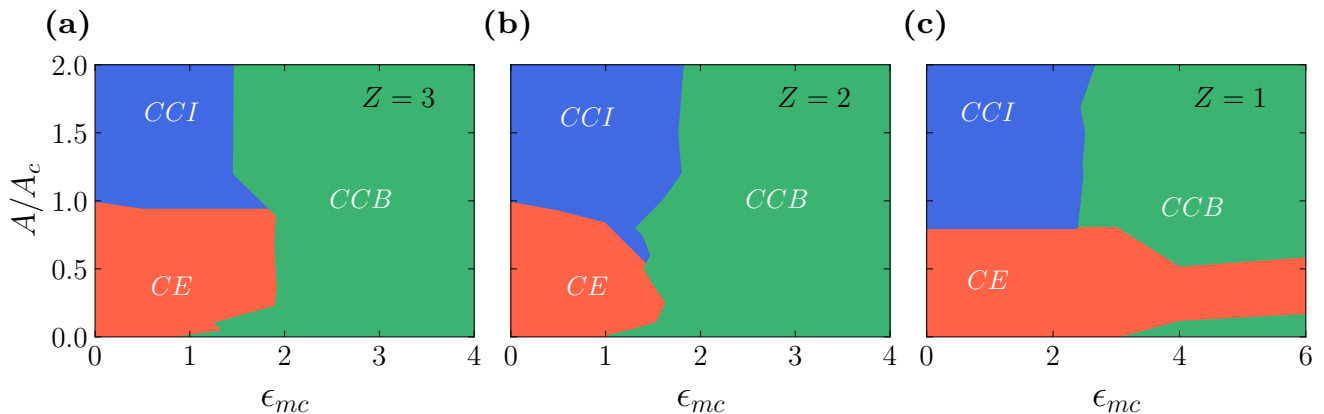


FIG. 10. The conformational phase-diagram of the PE in the A/A_c - ϵ_{mc} for (a) $Z = 3$, (b) $Z = 2$, and (c) $Z = 1$. The CE , CCI and CCB phases are represented in red, blue, and green colors respectively.

as CCB , observed for strong polymer-crowder attractive interactions, regardless of the charge density (at least for $Z = 2, 3$), facilitated by the crowders acting as bridges or crosslinks between the monomers.

Interestingly, the critical value of ϵ_{mc} required to induce the collapse of charged polymers (CE - CCB transition) with divalent and trivalent counterions is not significantly different from that observed for neutral polymers, as reported in our previous work⁶². However, we find that monovalent counterions exhibit distinct effects on the phases compared to multivalent counterions. In particular, for intermediate values of A , we find that the PE does not collapse for even quite large values of ϵ_{mc} . This may be due to steric effects which limits the number of crowders that can condense onto the PE. If this were true, then smaller sized crowders should induce a CE - CCB transition for intermediate values of A , because a larger number of crowders can be accommodated around the PE. Studying the effects of crowder size on the phase diagram is a promising area for future study.

Across the CE - CCB transition, the number of crowders increases substantially compared to the decrease in the number of condensed counterions, strongly suggesting that a much larger number of neutral crowders is required to collapse the charged PE to overcome the strong electrostatic repulsion. This difference in number of non-polymer particles inside the collapsed phase of the PE can lead to new subsets of collapsed phases, including swollen phases and can potentially affect the conformational landscape. The significant increase in attractive van der Waals interaction energy between the polymer and crowders also supports this notion.

We observe an intriguing phenomenon regarding the CCI - CCB phase boundary, which appears to remain largely unaffected by changes in A . This outcome is unexpected, as one would intuitively anticipate that for higher values of parameter A , the CCI phase's stability would strengthen, necessitating a correspondingly larger ϵ_{mc} to induce its destabilization. If A was indeed analogous to

ϵ_{mm} of neutral polymers, then it might be anticipated that the critical value of ϵ_{mc} (ϵ_{mc}^*) would exhibit a linear increase with A , as suggested by Garg et al.⁶². The independence of the CCI - CCB phase boundary on the variations in parameter A , holds particular significance in the context of theories surrounding the collapse of charged polymers. Various competing hypotheses, such as the ionic solid theory, dipole theory, and counterion fluctuation theory, have been posited to explain the counterintuitive collapse or aggregation of similarly charged polyelectrolytes (PEs)^{15,17–23,25,27,28,30–38,86,91,92}. In the dipole theory, the parameter A serves to enhance the effective value of ϵ_{mm} , thereby leading to the prediction of a linear relationship between ϵ_{mc}^* and A , which is in contradiction to our results. Our previous molecular dynamics simulations corroborate the counterion fluctuation theory, which argues that the emergent attractive forces are due to density fluctuations of densely packed counterions moving freely within the PE globule^{18–20,28}. How the inclusion of neutral crowders in the overall picture of PE with counterions affects the predictions of counterion fluctuation theory would be part of the future study. It is to be noted that, we previously showed the underlying mechanism that governs the aggregation of multiple similarly charged PEs when their charge densities exceed the critical threshold established for the collapse of an individual PE^{86,91,93}. Thus, the implications of understanding the role of neutral crowders for aggregation mechanism of multiple PEs would also be important to understand.

Moreover, the Flory-Huggins theory furnishes predictions regarding the conformational behavior of neutral polymers, accounting for diverse entropic and energetic factors influencing the free energy dynamics⁹⁴. However, the introduction of charges to the polymer structure necessitates the integration of electrostatic contributions into the free energy, accomplished through a Debye-Huckel term⁹⁵. Our previous work^{19,20} has demonstrated the requirement for additional terms within the virial ex-

pansion to comprehensively address the electrostatic influence on the free energy. The valency of counterions has a significant impact on the attractive volume interactions within the PE, as it determines the number of condensed counterions inside the collapsed PE globule²⁰. The introduction of attractive neutral crowders further complicates the scenario, as they compete with the condensed counterions, thereby enhancing the attractive interactions between the polymer and the crowders. These contrasting behaviors underscore the pivotal role played by the counterion valency in shaping the conformational landscape of charged polymers in the presence of neutral crowders. This can have profound implications for polymer models used for understanding phenomena such as chromatin organization and LLPS. Models such as strings and binders (SBS)^{74,96} or stickers-and-spacers⁹⁷ are simple neutral polymer models (lattice, mean field, etc.) used to describe chromatin organization, folding, or membraneless organelle formation via LLPS. These models primarily consider specific interactions with binding molecules, modeled as simple crowders. We expect significant changes to the understanding of these systems when the inherent charges of these biopolymers are incorporated, and the role of counterion valencies and the strength of soft attraction between biopolymers and crowders are modeled. Understanding how the introduction of charges in simple polymer models will affect the comparison with experimental Hi-C data will be part of future work.

V. SUPPLEMENTARY MATERIAL

Additional Data included.

ACKNOWLEDGMENTS

The simulations were carried out on the high performance computing machines Nandadevi at the Institute of Mathematical Sciences.

REFERENCES

- ¹G. C. Wong and L. Pollack, “Electrostatics of strongly charged biological polymers: ion-mediated interactions and self-organization in nucleic acids and proteins,” *Annual review of physical chemistry* **61**, 171–189 (2010).
- ²F. J. Solis and O. de la Cruz, “Collapse of flexible polyelectrolytes in multivalent salt solutions,” *J. Chem. Phys.* **112**, 2030–2035 (2000).
- ³A. Schneemann, “The structural and functional role of rna in icosahedral virus assembly,” *Ann. Rev. Microbiol.* **60**, 51–67 (2006).
- ⁴A. Siber, A. Losdorfer Bozic, and R. Podgornik, “Energies and pressures in viruses: contribution of non-specific electrostatic interactions,” *Phys. Chem. Chem. Phys.* **14**, 374–380 (2012).
- ⁵R. F. Bruinsma, M. Comas-Garcia, R. F. Garmann, and A. Y. Grosberg, “Equilibrium self-assembly of small rna viruses,” *Phys. Rev. E* **93**, 032405 (2016).
- ⁶P. van der Schoot and R. Bruinsma, “Electrostatics and the assembly of an rna virus,” *Phys. Rev. E* **71**, 061928 (2005).
- ⁷V. A. Bloomfield, “Condensation of dna by multivalent cations: Considerations on mechanism,” *Biopolymers* **31**, 1471–1481 (1991).
- ⁸V. A. Bloomfield, “Dna condensation,” *Curr. Opin. Struct. Biol.* **6**, 334–341 (1996).
- ⁹S. Mitragotri, D. G. Anderson, X. Chen, E. K. Chow, D. Ho, A. V. Kabanov, J. M. Karp, K. Kataoka, C. A. Mirkin, S. H. Petrosko, *et al.*, “Accelerating the translation of nanomaterials in biomedicine,” *ACS nano* **9**, 6644–6654 (2015).
- ¹⁰R. Russell, I. S. Millett, M. W. Tate, L. W. Kwok, B. Nakatani, S. M. Gruner, S. G. Mochrie, V. Pande, S. Doniach, D. Herschlag, *et al.*, “Rapid compaction during rna folding,” *Proceedings of the National Academy of Sciences* **99**, 4266–4271 (2002).
- ¹¹K. L. Buchmueller, A. E. Webb, D. A. Richardson, and K. M. Weeks, “A collapsed non-native rna folding state,” *Nature Structural & Molecular Biology* **7**, 362 (2000).
- ¹²V. L. Murthy and G. D. Rose, “Is counterion delocalization responsible for collapse in rna folding?” *Biochemistry* **39**, 14365–14370 (2000).
- ¹³R. Dias, A. Pais, M. Miguel, and B. Lindman, “Modeling of dna compaction by polycations,” *The Journal of chemical physics* **119**, 8150–8157 (2003).
- ¹⁴S. Chauhan and S. A. Woodson, “Tertiary interactions determine the accuracy of rna folding,” *Journal of the American Chemical Society* **130**, 1296–1303 (2008).
- ¹⁵G. S. Manning, “Limiting laws and counterion condensation in polyelectrolyte solutions i. colligative properties,” *The Journal of Chemical Physics* **51**, 924–933 (1969).
- ¹⁶G. S. Manning, “Condensation of counterions gives rise to contraction transitions in a one-dimensional polyelectrolyte gel,” *Polymers* **10**, 432 (2018).
- ¹⁷A. Varghese, S. Vemparala, and R. Rajesh, “Phase transitions of a single polyelectrolyte in a poor solvent with explicit counterions,” *The Journal of chemical physics* **135**, 154902 (2011).
- ¹⁸N. V. Brilliantov, D. V. Kuznetsov, and R. Klein, “Chain collapse and counterion condensation in dilute polyelectrolyte solutions,” *Phys. Rev. Lett.* **81**, 1433–1436 (1998).
- ¹⁹A. M. Tom, S. Vemparala, R. Rajesh, and N. V. Brilliantov, “Mechanism of chain collapse of strongly charged polyelectrolytes,” *Physical review letters* **117**, 147801 (2016).
- ²⁰A. M. Tom, S. Vemparala, R. Rajesh, and N. V. Brilliantov, “Regimes of electrostatic collapse of a highly charged polyelectrolyte in a poor solvent,” *Soft matter*

- 13**, 1862–1872 (2017).
- ²¹M. J. Stevens and K. Kremer, “Structure of salt-free linear polyelectrolytes,” *Phys. Rev. Lett.* **71**, 2228 (1993).
- ²²M. J. Stevens and K. Kremer, “The nature of flexible linear polyelectrolytes in salt free solution: A molecular dynamics study,” *The Journal of Chemical Physics* **103**, 1669–1690 (1995).
- ²³R. G. Winkler, M. Gold, and P. Reineker, “Collapse of polyelectrolyte macromolecules by counterion condensation and ion pair formation: A molecular dynamics simulation study,” *Phys. Rev. Lett.* **80**, 3731–3734 (1998).
- ²⁴S. M. Mel’nikov, M. O. Khan, B. Lindman, and B. Jönsson, “Phase behavior of single dna in mixed solvents,” *J. Am. Chem. Soc.* **121**, 1130–1136 (1999).
- ²⁵M. Deserno and C. Holm, “Theory and simulations of rigid polyelectrolytes,” *Mol. Phys.* **100**, 2941–2956 (2002).
- ²⁶A. Varghese, S. Vemparala, and R. Rajesh, “Phase transitions of a single polyelectrolyte in a poor solvent with explicit counterions,” *J. Chem. Phys.* **135**, 154902 (2011).
- ²⁷A. V. Dobrynin and M. Rubinstein, “Theory of polyelectrolytes in solutions and at surfaces,” *Prog. Poly. Science* **30**, 1049 – 1118 (2005).
- ²⁸A. A. Gavrillov, A. V. Chertovich, and E. Y. Kramarenko, “Conformational behavior of a single polyelectrolyte chain with bulky counterions,” *Macromolecules* **49**, 1103–1110 (2016).
- ²⁹A. A. Gavrillov, A. V. Chertovich, and E. Y. Kramarenko, “Dissipative particle dynamics for systems with high density of charges: Implementation of electrostatic interactions,” *J. Chem. Phys.* **145**, 174101 (2016).
- ³⁰V. A. Bloomfield, “Dna condensation by multivalent cations,” *Biopolymers: Original Research on Biomolecules* **44**, 269–282 (1997).
- ³¹A. Cherstvy, “Collapse of highly charged polyelectrolytes triggered by attractive dipole-dipole and correlation-induced electrostatic interactions,” *The Journal of Physical Chemistry B* **114**, 5241–5249 (2010).
- ³²Y. D. Gordievskaya, Y. A. Budkov, and E. Y. Kramarenko, “An interplay of electrostatic and excluded volume interactions in the conformational behavior of a dipolar chain: theory and computer simulations,” *Soft matter* **14**, 3232–3235 (2018).
- ³³M. Muthukumar, “Theory of counter-ion condensation on flexible polyelectrolytes: Adsorption mechanism,” *The Journal of chemical physics* **120**, 9343–9350 (2004).
- ³⁴F. J. Solis and M. O. De La Cruz, “Collapse of flexible polyelectrolytes in multivalent salt solutions,” *The Journal of Chemical Physics* **112**, 2030–2035 (2000).
- ³⁵A. Y. Grosberg and A. R. Khokhlov, *Statistical Physics of Macromolecules* (AIP Press, Woodbury, NY, 1994).
- ³⁶S. M. Mel’nikov, M. O. Khan, B. Lindman, and B. Jönsson, “Phase behavior of single dna in mixed solvents,” *J. Am. Chem. Soc.* **121**, 1130–1136 (1999).
- ³⁷A. R. Khokhlov, “On the collapse of weakly charged polyelectrolytes,” *J. Phys. A* **13**, 979–987 (1980).
- ³⁸H. Schiessel and P. Pincus, “Counterion-condensation-induced collapse of highly charged polyelectrolytes,” *Macromolecules* **31**, 7953–7959 (1998).
- ³⁹G. Rivas, F. Ferrone, and J. Herzfeld, “Life in a crowded world: Workshop on the biological implications of macromolecular crowding,” (2004).
- ⁴⁰H.-X. Zhou, G. Rivas, and A. P. Minton, “Macromolecular crowding and confinement: biochemical, biophysical, and potential physiological consequences,” *Annu. Rev. Biophys.* **37**, 375–397 (2008).
- ⁴¹G. Rivas and A. P. Minton, “Macromolecular crowding in vitro, in vivo, and in between,” *Trends in biochemical sciences* **41**, 970–981 (2016).
- ⁴²S. B. Zimmerman and S. O. Trach, “Estimation of macromolecule concentrations and excluded volume effects for the cytoplasm of escherichia coli,” *Journal of molecular biology* **222**, 599–620 (1991).
- ⁴³R. J. Ellis and A. P. Minton, “Join the crowd,” *Nature* **425**, 27–28 (2003).
- ⁴⁴R. J. Ellis, “Macromolecular crowding: an important but neglected aspect of the intracellular environment,” *Current opinion in structural biology* **11**, 114–119 (2001).
- ⁴⁵S. B. Zimmerman and A. P. Minton, “Macromolecular crowding: biochemical, biophysical, and physiological consequences,” *Annual review of biophysics and biomolecular structure* **22**, 27–65 (1993).
- ⁴⁶D. Nayar, “Small crowder interactions can drive hydrophobic polymer collapse as well as unfolding,” *Physical Chemistry Chemical Physics* **22**, 18091–18101 (2020).
- ⁴⁷R. Zangi, R. Zhou, and B. Berne, “Urea’s action on hydrophobic interactions,” *Journal of the American Chemical Society* **131**, 1535–1541 (2009).
- ⁴⁸W. M. Mardoum, S. M. Gorczyca, K. E. Regan, T.-C. Wu, and R. M. Robertson-Anderson, “Crowding induces entropically-driven changes to dna dynamics that depend on crowder structure and ionic conditions,” *Frontiers in physics* **6**, 53 (2018).
- ⁴⁹S.-i. Nakano and N. Sugimoto, “Model studies of the effects of intracellular crowding on nucleic acid interactions,” *Molecular BioSystems* **13**, 32–41 (2017).
- ⁵⁰J. Shin, A. G. Cherstvy, and R. Metzler, “Kinetics of polymer looping with macromolecular crowding: effects of volume fraction and crowder size,” *Soft matter* **11**, 472–488 (2015).
- ⁵¹X. Liu, H. Jiang, and Z. Hou, “Non-monotonic dependence of polymer chain dynamics on active crowder size,” *The Journal of Chemical Physics* **152**, 204906 (2020).
- ⁵²M. P. Taylor, C. Vinci, and R. Suzuki, “Effects of macromolecular crowding on the folding of a polymer chain: A wang-landau simulation study,” *The Journal*

- of Chemical Physics **153**, 174901 (2020).
- ⁵³S. Asakura and F. Oosawa, “On interaction between two bodies immersed in a solution of macromolecules,” *The Journal of chemical physics* **22**, 1255–1256 (1954).
- ⁵⁴S. Asakura and F. Oosawa, “Interaction between particles suspended in solutions of macromolecules,” *Journal of polymer science* **33**, 183–192 (1958).
- ⁵⁵D. Nayar, “Molecular crowders can induce collapse in hydrophilic polymers via soft attractive interactions,” *The Journal of Physical Chemistry B* (2023).
- ⁵⁶M. Mukherjee and J. Mondal, “Osmolyte-induced collapse of a charged macromolecule,” *The Journal of Physical Chemistry B* **123**, 4636–4644 (2019).
- ⁵⁷K. Tripathi, G. I. Menon, and S. Vemparala, “Confined crowded polymers near attractive surfaces,” *The Journal of Chemical Physics* **151** (2019), 244901.
- ⁵⁸K. Tripathi and S. Vemparala, “Conformational landscape of long semiflexible linear and ring polymers near attractive surfaces,” (2023), arXiv:2304.11548 [cond-mat.soft].
- ⁵⁹K. Miyazaki, K. Schweizer, D. Thirumalai, R. Tunier, and E. Zaccarelli, “The asakura–oosawa theory: Entropic forces in physics, biology, and soft matter,” (2022).
- ⁶⁰R. Bhat and S. N. Timasheff, “Steric exclusion is the principal source of the preferential hydration of proteins in the presence of polyethylene glycols,” *Protein Science* **1**, 1133–1143 (1992).
- ⁶¹H. Kang, P. A. Pincus, C. Hyeon, and D. Thirumalai, “Effects of macromolecular crowding on the collapse of biopolymers,” *Physical review letters* **114**, 068303 (2015).
- ⁶²H. Garg, R. Rajesh, and S. Vemparala, “The conformational phase diagram of neutral polymers in the presence of attractive crowders,” *The Journal of Chemical Physics* **158** (2023).
- ⁶³D. Antypov and J. A. Elliott, “Computer simulation study of a single polymer chain in an attractive solvent,” *The Journal of chemical physics* **129**, 174901 (2008).
- ⁶⁴J. Heyda, A. Muzdalo, and J. Dzubiella, “Rationalizing polymer swelling and collapse under attractive cosolvent conditions,” *Macromolecules* **46**, 1231–1238 (2013).
- ⁶⁵F. Rodríguez-Roperó, T. Hajari, and N. F. van der Vegt, “Mechanism of polymer collapse in miscible good solvents,” *The Journal of Physical Chemistry B* **119**, 15780–15788 (2015).
- ⁶⁶Y. Huang and S. Cheng, “Chain conformations and phase separation in polymer solutions with varying solvent quality,” *Journal of Polymer Science* **59**, 2819–2831 (2021).
- ⁶⁷F. Erdel and K. Rippe, “Formation of chromatin subcompartments by phase separation,” *Biophysical journal* **114**, 2262–2270 (2018).
- ⁶⁸J. T. King and A. Shakya, “Phase separation of dna: From past to present,” *Biophysical Journal* **120**, 1139–1149 (2021).
- ⁶⁹J.-K. Ryu, D.-E. Hwang, and J.-M. Choi, “Current understanding of molecular phase separation in chromosomes,” *International Journal of Molecular Sciences* **22**, 10736 (2021).
- ⁷⁰C. A. Azaldegui, A. G. Vecchiarelli, and J. S. Biteen, “The emergence of phase separation as an organizing principle in bacteria,” *Biophysical journal* **120**, 1123–1138 (2021).
- ⁷¹J.-K. Ryu, C. Bouchoux, H. W. Liu, E. Kim, M. Minamino, R. de Groot, A. J. Katan, A. Bonato, D. Marenduzzo, D. Michieletto, *et al.*, “Bridging-induced phase separation induced by cohesin smc protein complexes,” *Science Advances* **7**, eabe5905 (2021).
- ⁷²C. Brackley, “Polymer compaction and bridging-induced clustering of protein-inspired patchy particles,” *Journal of Physics: Condensed Matter* **32**, 314002 (2020).
- ⁷³C. A. Brackley, S. Taylor, A. Papantonis, P. R. Cook, and D. Marenduzzo, “Nonspecific bridging-induced attraction drives clustering of dna-binding proteins and genome organization,” *Proceedings of the National Academy of Sciences* **110**, E3605–E3611 (2013).
- ⁷⁴M. Barbieri, M. Chotalia, J. Fraser, L.-M. Lavitas, J. Dostie, A. Pombo, and M. Nicodemi, “Complexity of chromatin folding is captured by the strings and binders switch model,” *Proceedings of the National Academy of Sciences* **109**, 16173–16178 (2012).
- ⁷⁵D. Murugesapillai, M. J. McCauley, R. Huo, M. H. Nelson Holte, A. Stepanyants, L. J. Maher III, N. E. Israeloff, and M. C. Williams, “Dna bridging and looping by hmo1 provides a mechanism for stabilizing nucleosome-free chromatin,” *Nucleic acids research* **42**, 8996–9004 (2014).
- ⁷⁶S. Machida, Y. Takizawa, M. Ishimaru, Y. Sugita, S. Sekine, J.-i. Nakayama, M. Wolf, and H. Kurumizaka, “Structural basis of heterochromatin formation by human hp1,” *Molecular cell* **69**, 385–397 (2018).
- ⁷⁷I. Malhotra, B. Oyarzún, and B. M. Mognetti, “Unfolding of the chromatin fiber driven by overexpression of noninteracting bridging factors,” *Biophysical journal* **120**, 1247–1256 (2021).
- ⁷⁸C. A. Brackley and D. Marenduzzo, “Bridging-induced microphase separation: photobleaching experiments, chromatin domains and the need for active reactions,” *Briefings in functional genomics* **19**, 111–118 (2020).
- ⁷⁹S. Biedzinski, B. Parmar, and S. C. Weber, “Beyond equilibrium phase diagrams: enzymatic activity shakes up bacterial condensates,” *Molecular cell* **79**, 205–206 (2020).
- ⁸⁰S. Plimpton, “Fast parallel algorithms for short-range molecular dynamics,” *Journal of computational physics* **117**, 1–19 (1995).
- ⁸¹L. Verlet, “Computer” experiments” on classical fluids. i. thermodynamical properties of lennard-jones molecules,” *Physical review* **159**, 98 (1967).
- ⁸²W. C. Swope, H. C. Andersen, P. H. Berens, and K. R. Wilson, “A computer simulation method for the calculation of equilibrium constants for the formation of

- physical clusters of molecules: Application to small water clusters,” *The Journal of Chemical Physics* **76**, 637–649 (1982).
- ⁸³S. Nosé, “A unified formulation of the constant temperature molecular dynamics methods,” *The Journal of chemical physics* **81**, 511–519 (1984).
- ⁸⁴W. G. Hoover, “Canonical dynamics: Equilibrium phase-space distributions,” *Physical review A* **31**, 1695 (1985).
- ⁸⁵R. W. Hockney and J. W. Eastwood, *Computer simulation using particles* (crc Press, 2021).
- ⁸⁶A. M. Tom, R. Rajesh, and S. Vemparala, “Aggregation of flexible polyelectrolytes: Phase diagram and dynamics,” *The Journal of chemical physics* **147**, 144903 (2017).
- ⁸⁷R. I. Dima, “Asymmetry in the shapes of folded and denatured states of proteins,” *The Journal of Physical Chemistry B* **108**, 6564–6570 (2004).
- ⁸⁸D. N. Theodorou and U. W. Suter, “Shape of unperturbed linear polymers: polypropylene,” *Macromolecules* **18**, 1206–1214 (1985).
- ⁸⁹A. P. Minton, “Excluded volume as a determinant of macromolecular structure and reactivity,” *Biopolymers: Original Research on Biomolecules* **20**, 2093–2120 (1981).
- ⁹⁰S. L. Speer, C. J. Stewart, L. Sapir, D. Harries, and G. J. Pielak, “Macromolecular crowding is more than hard-core repulsions,” *Annual Review of Biophysics* **51**, 267–300 (2022).
- ⁹¹A. M. Tom, R. Rajesh, and S. Vemparala, *J. of Chem. Phys.* **144**, 034904 (2016).
- ⁹²A. Varghese, R. Rajesh, and S. Vemparala, “Aggregation of rod-like polyelectrolyte chains in the presence of monovalent counterions,” *The Journal of chemical physics* **137**, 234901 (2012).
- ⁹³A. Varghese, R. Rajesh, and S. Vemparala, “Aggregation of rod-like polyelectrolyte chains in the presence of monovalent counterions,” *J. of Chem. Phys.* **137**, 234901 (2012).
- ⁹⁴P.-G. De Gennes and P.-G. Gennes, *Scaling concepts in polymer physics* (Cornell university press, 1979).
- ⁹⁵J. T. G. Overbeek and M. Voorn, “Phase separation in polyelectrolyte solutions. theory of complex coacervation,” *Journal of Cellular and Comparative Physiology* **49**, 7–26 (1957).
- ⁹⁶A. M. Chiariello, C. Annunziatella, S. Bianco, A. Esposito, and M. Nicodemi, “Polymer physics of chromosome large-scale 3d organisation,” *Scientific reports* **6**, 29775 (2016).
- ⁹⁷J.-M. Choi, A. S. Holehouse, and R. V. Pappu, “Physical principles underlying the complex biology of intracellular phase transitions,” *Annual review of biophysics* **49**, 107–133 (2020).